MULTIBODY DYNAMICS 2009, ECCOMAS Thematic Conference
K. Arczewski, J. Frączek, M. Wojtyra (eds.)
Warsaw, Poland, 29 June – 2 July 2009

INFLUENCE OF THE SENSORED MAGNITUDE IN THE PERFORMANCE OF OBSERVERS BASED ON MULTIBODY MODELS AND THE EXTENDED KALMAN FILTER

Javier Cuadrado*, Daniel Dopico*, Jose A. Perez* and Roland Pastorino*

* Escuela Politecnica Superior
University of La Coruña, Mendizabal s/n, 15403 Ferrol, Spain
e-mail: javicuad@cdf.udc.es,
web page: http://lim.ii.udc.es

Keywords: State Estimation, Detailed Multibody Models, Extended Kalman Filter, Sensors, Control, State-Space Reduction Method, Efficient Formalisms, Real-Time Applications.

Abstract. *This work is part of a project aimed to develop real-time observers based on detailed multibody models and the extended Kalman filter (EKF). Detailed models can provide more and more accurate information than the simple models traditionally used to build observers, thus enabling the implementation of more sophisticated control strategies. In a previous work, the authors studied different multibody dynamics formulations, and concluded that the state-space reduction method known as matrix-R was the most suitable for this application. This second work is devoted to study the influence of the sensored magnitude in the performance of the observers. Although the final objective is to address complex industrial systems, preliminary studies are being carried out on a four-bar mechanism with a spring-damper element. The behavior of the matrix-R method has been analyzed for different sensored magnitudes -position, velocity, acceleration-, and for the cases when the sensored magnitude is or is not a generalized coordinate of the problem. The conclusion is that good results can be obtained in all the cases, provided the covariance of the measurement noise is adjusted to a suitable value.*

1 INTRODUCTION

Observers serve to estimate the states of a dynamic system based on a model and on some measurements of the system [1]. In this way, they provide estimates of magnitudes which have not been sensored because it would be either expensive or practically difficult. In many cases, observers must run in real-time, since the information they provide is used to control the actual system.

Usually, the system models are simple, even linear, since their fast evaluation is needed in order to meet the above mentioned real-time requirement. However, detailed models would provide more and more accurate information, thus enabling the implementation of more sophisticated control strategies.

This work is part of a project aimed to develop real-time observers based on detailed multibody models and the extended Kalman filter (EKF). Although the objective is to address complex industrial systems, preliminary studies are being carried out on a four-bar mechanism with a spring-damper element.

In a previous work [2], the authors selected the two dynamic formulations which were found to better fit the structure required by the EKF, and compared them: a state-space reduction method known as matrix-R method, and a penalty method. It was concluded that the matrix-R method was faster and more accurate than its counterpart. The penalty method was not able to keep constraint satisfaction, since an increment of the penalty factor increased both the penalty forces which oppose constraint violation and the correction terms coming from the EKF. Therefore, the kinematic position and velocity problems had to be solved at every function evaluation, thus limiting the efficiency of the method and its typical advantages: validity of the set of variables during the whole simulation, even in case of changing configurations, and robustness when facing singular positions.

This second work is devoted to study the influence of the sensored magnitude in the performance of the observers. In the above-mentioned first work, a position sensor had been considered which measured the value of the generalized coordinate. Here, the behavior of the matrix-R method has been analyzed for different sensored magnitudes -position, velocity, acceleration-, and for the cases when the sensored magnitude is or is not a generalized coordinate of the problem.

2 THE OBSERVER BASED ON THE MATRIX-R METHOD AND THE EKF

Consider the nonlinear system (plant) given by:

$$\begin{aligned} \dot{\mathbf{x}} &= \mathbf{f}(\mathbf{x}) + \boldsymbol{\delta} \\ \mathbf{y} &= \mathbf{h}(\mathbf{x}) + \boldsymbol{\varepsilon} \end{aligned} \tag{1}$$

where $\mathbf{x}$ is the (unknown) state vector, and $\mathbf{y}$ is the known measurements vector. The functions $\mathbf{f}$ and $\mathbf{h}$ are also known, and the equations are affected by state and measurement noises $\boldsymbol{\delta}$, $\boldsymbol{\varepsilon}$, with zero mean and given covariances $\boldsymbol{\Theta}$, $\boldsymbol{\Xi}$, respectively. Then, the EKF is given by [3]:

$$\begin{aligned} \dot{\hat{\mathbf{x}}} &= \mathbf{f}(\hat{\mathbf{x}}, \mathbf{u}) + \mathfrak{K}\left(\mathbf{y} - \mathbf{h}(\hat{\mathbf{x}})\right) \\ \mathfrak{K} &= \mathbf{P}\mathfrak{C}^{\mathrm{T}}\boldsymbol{\Xi}^{-1} \\ \dot{\mathbf{P}} &= \mathfrak{A}\mathbf{P} + \mathbf{P}\mathfrak{A}^{\mathrm{T}} - \mathbf{P}\mathfrak{C}^{\mathrm{T}}\boldsymbol{\Xi}^{-1}\mathfrak{C}\mathbf{P} + \boldsymbol{\Theta} \end{aligned} \tag{2}$$

being the matrices $\mathfrak{A}$, $\mathfrak{C}$, computed as the Jacobians of **f** and **h** with respect to the states, and evaluated at the estimated trajectory. The EKF locally minimizes the covariance **P** of the state-estimation error.

In its most basic form, the dynamics of a multibody system is described by the constrained Lagrangian equations:

$$\begin{aligned} \mathbf{M}\ddot{\mathbf{q}} + \boldsymbol{\Phi}_{\mathbf{q}}^{\mathrm{T}}\boldsymbol{\lambda} &= \mathbf{Q} \\ \boldsymbol{\Phi} &= \mathbf{0} \end{aligned} \tag{3}$$

where **M** is the positive semidefinite mass matrix, $\ddot{\mathbf{q}}$ the accelerations vector, $\boldsymbol{\Phi}$ the constraints vector, $\boldsymbol{\Phi}_{\mathbf{q}}$ the Jacobian matrix of the constraints, $\boldsymbol{\lambda}$ the Lagrange multipliers vector, and **Q** the applied forces vector. Eq. (1) represents a system of differential-algebraic equations (DAE).

The main idea of the matrix-R method [4] is to obtain a system of ordinary differential equations (ODE) with dimension n_i equal to the actual number of degrees of freedom, using a set **z** of independent coordinates. The starting point is to establish the following relation between velocities:

$$\dot{\mathbf{q}} = \mathbf{R}\dot{\mathbf{z}} \tag{4}$$

where **q** are all the n_d dependent variables and **z** is a set of n_i independent variables. Such a relation can always be found, for instance, taking the derivative of the constraints, $\boldsymbol{\Phi}_{\mathbf{q}}\dot{\mathbf{q}} = \mathbf{0}$, and splitting all the velocities in two subsets, so that one subset of velocities may be written as a function of the other subset. Once Eq. (4) is obtained, it follows that

$$\ddot{\mathbf{q}} = \mathbf{R}\ddot{\mathbf{z}} + \dot{\mathbf{R}}\dot{\mathbf{z}} \tag{5}$$

Going back to Eq. (3), premultiplying by the transpose of **R**, and having in mind that $\boldsymbol{\Phi}_{\mathbf{q}}\mathbf{R} = \mathbf{0}$,

$$\ddot{\mathbf{z}} = \left(\mathbf{R}^{\mathrm{T}}\mathbf{M}\mathbf{R}\right)^{-1}\left[\mathbf{R}^{\mathrm{T}}\left(\mathbf{Q} - \mathbf{M}\dot{\mathbf{R}}\dot{\mathbf{z}}\right)\right] = \bar{\mathbf{M}}^{-1}\bar{\mathbf{Q}} \tag{6}$$

which defines the projected mass matrix $\bar{\mathbf{M}}$ and the projected vector of generalized forces $\bar{\mathbf{Q}}$. The result is that the DAE of Eq. (3) in the dependent variables has been converted into the ODE of Eq. (6) expressed in independent variables.

If now the states are defined as $\mathbf{x}^{\mathrm{T}} = \left\{\mathbf{z}^{\mathrm{T}} \;\; \mathbf{w}^{\mathrm{T}}\right\}$, with $\mathbf{w} = \dot{\mathbf{z}}$, the following equations can be written,

$$\begin{aligned} \dot{\mathbf{z}} &= \mathbf{w} \\ \dot{\mathbf{w}} &= \left(\mathbf{R}^{\mathrm{T}}\mathbf{M}\mathbf{R}\right)^{-1}\left[\mathbf{R}^{\mathrm{T}}\left(\mathbf{Q} - \mathbf{M}\dot{\mathbf{R}}\mathbf{w}\right)\right] = \bar{\mathbf{M}}^{-1}\bar{\mathbf{Q}} \end{aligned} \tag{7}$$

or, more compactly,

$$\begin{Bmatrix} \dot{\mathbf{z}} \\ \dot{\mathbf{w}} \end{Bmatrix} = \begin{Bmatrix} \mathbf{w} \\ \bar{\mathbf{M}}^{-1}\bar{\mathbf{Q}} \end{Bmatrix} \;\Rightarrow\; \dot{\mathbf{x}} = \mathbf{f}(\mathbf{x}) \tag{8}$$

These equations perfectly match the first set of Eq. (1) and, therefore, the EKF of Eq. (2) can be straightforwardly applied. In particular, the state-space matrix is obtained as the linearization:

$$\mathfrak{A}=\frac{\partial \mathbf{f}(\mathbf{x})}{\partial \mathbf{x}}=\begin{bmatrix} \mathbf{0} & \mathbf{I} \\ \dfrac{\partial\left(\bar{\mathbf{M}}^{-1}\bar{\mathbf{Q}}\right)}{\partial \mathbf{z}} & \dfrac{\partial\left(\bar{\mathbf{M}}^{-1}\bar{\mathbf{Q}}\right)}{\partial \mathbf{w}} \end{bmatrix} \tag{9}$$

which can be approximated as,

$$\begin{aligned} \mathfrak{A}&=\begin{bmatrix} \mathbf{0} & \mathbf{I} \\ \mathfrak{A}_{21} & \mathfrak{A}_{22} \end{bmatrix} \\ \mathfrak{A}_{21}&=-\bar{\mathbf{M}}^{-1}\mathbf{R}^{\mathrm{T}}\left(\mathbf{K}\mathbf{R}+2\mathbf{M}\mathbf{R}_{\mathbf{q}}\mathbf{R}\dot{\mathbf{w}}\right) \\ \mathfrak{A}_{22}&=-\bar{\mathbf{M}}^{-1}\mathbf{R}^{\mathrm{T}}\left(\mathbf{C}\mathbf{R}+\mathbf{M}\dot{\mathbf{R}}\right) \end{aligned} \tag{10}$$

where $\mathbf{K}$ is the stiffness matrix and $\mathbf{C}$ is the damping matrix.

In this case, the size of the problem is $2n_i$. Now, according to Eq. (2), the correction provided by the EKF must be included into the observer equations,

$$\begin{aligned} \dot{\mathbf{z}}-\mathbf{w}+\mathfrak{K}_1\left(\mathbf{y}-\mathbf{y}_{\mathbf{s}}\right)&=\mathbf{0} \\ \bar{\mathbf{M}}\dot{\mathbf{w}}-\bar{\mathbf{Q}}+\bar{\mathbf{M}}\mathfrak{K}_2\left(\mathbf{y}-\mathbf{y}_{\mathbf{s}}\right)&=\mathbf{0} \end{aligned} \tag{11}$$

where $\mathfrak{K}_1$ and $\mathfrak{K}_2$ are the upper and lower parts of the Kalman gain matrix $\mathfrak{K}$, and $\mathbf{y}_{\mathbf{s}}$ are the outputs provided by the sensors.

Since real-time performance of the algorithms will be required by the final applications, the integration procedure is relevant in order to make the algorithm as efficient as possible. The implicit single-step trapezoidal rule has been selected as integrator,

$$\begin{aligned} \dot{\mathbf{z}}_{n+1}&=\frac{2}{\Delta t}\mathbf{z}_{n+1}-\left(\frac{2}{\Delta t}\mathbf{z}_n+\dot{\mathbf{z}}_n\right) \\ \dot{\mathbf{w}}_{n+1}&=\frac{2}{\Delta t}\mathbf{w}_{n+1}-\left(\frac{2}{\Delta t}\mathbf{w}_n+\dot{\mathbf{w}}_n\right) \end{aligned} \tag{12}$$

Now, Eq. (12) can be substituted into Eq. (11), thus leading to the nonlinear system of equations in the states,

$$\begin{cases} \mathbf{g}_1(\mathbf{x}_{n+1})=\mathbf{0} \\ \mathbf{g}_2(\mathbf{x}_{n+1})=\mathbf{0} \end{cases} \quad \Rightarrow \quad \mathbf{g}(\mathbf{x}_{n+1})=\mathbf{0} \tag{13}$$

This system can be iteratively solved by the Newton-Raphson iteration, the approximated tangent matrix being,

$$\frac{\partial \mathbf{g}}{\partial \mathbf{x}}=\begin{bmatrix} \dfrac{2}{\Delta t}\mathbf{I} & -\mathbf{I} \\ \mathbf{R}^{\mathrm{T}}\mathbf{K}\mathbf{R} & \mathbf{R}^{\mathrm{T}}(\mathbf{C}\mathbf{R}+\mathbf{M}\dot{\mathbf{R}})+\dfrac{2}{\Delta t}\bar{\mathbf{M}} \end{bmatrix}+\begin{bmatrix} \mathfrak{K}_1\mathfrak{C}_1 & \mathfrak{K}_1\mathfrak{C}_2 \\ \bar{\mathbf{M}}\mathfrak{K}_2\mathfrak{C}_1 & \bar{\mathbf{M}}\mathfrak{K}_2\mathfrak{C}_2 \end{bmatrix} \tag{14}$$

where $\mathfrak{C}_1$ and $\mathfrak{C}_2$ are the upper and lower parts of the output Jacobian matrix $\mathfrak{C}$.

3 THE EXAMPLE

The four-bar mechanism with a spring-damper element shown in Fig. (1) is chosen as example. Two computational versions of the mechanism are created: the first one represents the real "prototype", while the second one plays the role of the "model". In order to test the observer, the model is not an exact replica of the prototype, but differs in some physical or geometric parameters; also, the readings coming from sensors and actuators may be altered when passed to the model. The objective is that the model follows the motion of the prototype with the help of the EKF corrections.

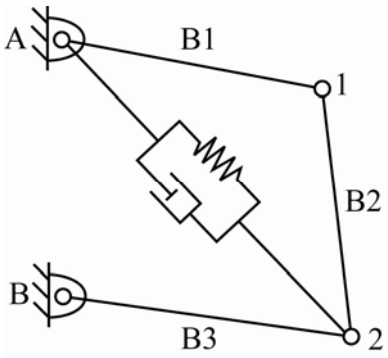

Figure 1: Four-bar mechanism with spring-damper element.

The following set of dependent variables, whose meaning is illustrated in Fig. (2), is used to model the mechanism:

$$\mathbf{q}^{\mathrm{T}} = \{x_1 \quad y_1 \quad x_2 \quad y_2 \quad s \quad \theta\} \tag{15}$$

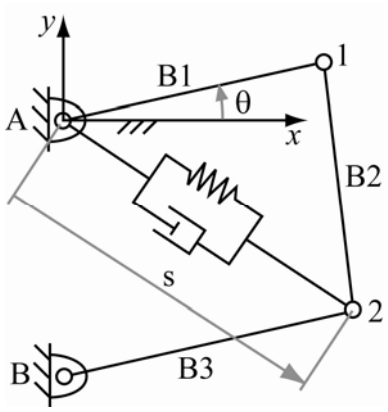

Figure 2: Modeling of the example.

The independent variable describing the single degree-of-freedom of the system is the angle between the horizontal and the link B1,

$$\mathbf{z}^{\mathrm{T}} = \{\theta\} \tag{16}$$

The inertial matrix of the whole mechanism is computed by considering the contributions of the three 2D bars [4] and the null contribution of the spring-damper element (of negligible mass):

$$\mathbf{M}=\begin{bmatrix} \frac{m_{B1}+m_{B2}}{3} & 0 & \frac{m_{B2}}{6} & 0 & 0\ 0 \\ 0 & \frac{m_{B1}+m_{B2}}{3} & 0 & \frac{m_{B2}}{6} & 0\ 0 \\ \frac{m_{B2}}{6} & 0 & \frac{m_{B2}+m_{B3}}{3} & 0 & 0\ 0 \\ 0 & \frac{m_{B2}}{6} & 0 & \frac{m_{B2}+m_{B3}}{3} & 0\ 0 \\ 0 & 0 & 0 & 0 & 0\ 0 \\ 0 & 0 & 0 & 0 & 0\ 0 \end{bmatrix} \tag{17}$$

The generalized force vector is obtained by considering the gravity that acts over each bar and the action of the spring-damper element, thus resulting [4]:

$$\mathbf{Q}=\begin{Bmatrix} 0 \\ -\frac{m_{B1}g}{2}-\frac{m_{B2}g}{2} \\ 0 \\ -\frac{m_{B2}g}{2}-\frac{m_{B3}g}{2} \\ -k\left(s-s_0\right)-c\dot{s} \\ 0 \end{Bmatrix} \tag{18}$$

where k is the elastic constant, c the damping coefficient and s_0 the natural spring length.

Finally, the constraints vector is:

$$\mathbf{\Phi}=\begin{Bmatrix} \left(x_1-x_A\right)^2+\left(y_1-y_A\right)^2-L_{B1}^2 \\ \left(x_2-x_1\right)^2+\left(y_2-y_1\right)^2-L_{B2}^2 \\ \left(x_2-x_B\right)^2+\left(y_2-y_B\right)^2-L_{B3}^2 \\ \left(x_2-x_A\right)^2+\left(y_2-y_A\right)^2-s^2 \\ y_1-L_{B1}\sin\theta \end{Bmatrix} \tag{19}$$

The numerical values of the parameters are: masses m_{B1}=2 kg, m_{B2}=25 kg, m_{B3}=2 kg; bar lengths L_{B1}=0.9 m, L_{B2}=1 m, L_{B3}=1.05 m; natural spring length s_0=1.4 m; fixed points Cartesian coordinates A=(0,0), B=(0,–1); spring coefficient k=10000 N/m, and damping coefficient c=500 Ns/m.

As said at the beginning of the section, two versions of the mechanism are created, the "prototype" and the "model", whose differences are: to show the recovery from different initial conditions, the real prototype starts at s=1.80 m, while the observer starts at s=1.85 m; to evaluate the effect of noise in measurements, a uniformly distributed sensor noise of 10% of the RMS value of the corresponding signal is considered; finally, in order to check the effect of uncertain exogenous forces, the prototype runs under normal gravity, g=9.81 m/s^2, but the observer runs under g=8.81 m/s^2. Both the prototype and the observer (model with EKF corrections) are simulated for a total time of 1 s.

Based on the experience obtained with the same example in the previous work [2], the EKF parameters are set as follows: covariance of the state noise, $\boldsymbol{\Theta}$=diag(10); covariance of the state estimation error, $\mathbf{P}(0)$=diag(diag(0.1),diag(0)). The covariance of the measurement noise, $\boldsymbol{\Xi}$, must be adjusted depending on the sensored magnitude.

4 THE INVESTIGATION

The investigation is organized as follows. To begin with, two main monitoring options have been considered: in the first one, the sensor measures the angle between the horizontal and the link B1, called θ; in the second one, the sensor measures the vertical coordinate of point 1, called y_1.

For each option, the sensored magnitude may be the position, velocity or acceleration of the corresponding variable, i.e. the possible sensored quantities are θ, $\dot{\theta}$, $\ddot{\theta}$ for the first option, and y_1, $\dot{y}_1$, $\ddot{y}_1$ for the second option. It should be pointed out that, since angle θ is the generalized coordinate of the problem, as indicated in Eq. (16), simpler expressions are obtained for the Jacobian $\mathbb{C}$ (see Eq. (1-2)) when θ or its derivatives are measured. In fact, if θ or $\dot{\theta}$ are the sensored quantities, $\mathbb{C}$ is constant.

Table 1 shows the different cases analyzed, and the value of the Jacobian of the measurements function, $\mathbb{C}$, for each of them. To interpret the table according to the formulation described in Section 2, it should be taken into account that $z=\theta$, $w=\dot{\theta}$, $\dot{w}=\ddot{\theta}$, and the form of the scalar terms $\mathcal{A}_{21}$, $\mathcal{A}_{22}$ is obtained from Eq. (10).

Sensor	$\mathbb{C}=\dfrac{\partial \mathbf{h}(\mathbf{x})}{\partial \mathbf{x}}$
θ	$\begin{bmatrix}1 & 0\end{bmatrix}$
$\dot{\theta}$	$\begin{bmatrix}0 & 1\end{bmatrix}$
$\ddot{\theta}$	$\begin{bmatrix}\mathcal{A}_{21} & \mathcal{A}_{22}\end{bmatrix}$
y_1	$\begin{bmatrix}L_{B1}\cos\theta & 0\end{bmatrix}$
$\dot{y}_1$	$L_{B1}\begin{bmatrix}-\dot{\theta}\sin\theta & \cos\theta\end{bmatrix}$
$\ddot{y}_1$	$L_{B1}\begin{bmatrix}-\ddot{\theta}\sin\theta+\mathcal{A}_{21}\cos\theta-\dot{\theta}^2\cos\theta & \mathcal{A}_{22}\cos\theta-2\dot{\theta}\sin\theta\end{bmatrix}$

Table 1: The different cases analyzed, and their $\mathbb{C}$ matrices.

Apart from what has been described above, two additional options have been considered in the study.

On the one hand, it has been supposed that the sensor at point 1 provides the measured values in local coordinates, as sensors usually do. Only two cases are meaningful within this approach, corresponding to the measurement of $\bar{y}_1$ and $\ddot{\bar{y}}_1$, respectively. However, in such cases the Jacobians of the measurement functions are $\mathbb{C}=L_{B1}\begin{bmatrix}0 & 1\end{bmatrix}$ and $\mathbb{C}=L_{B1}\begin{bmatrix}\mathcal{A}_{21} & \mathcal{A}_{22}\end{bmatrix}$, which show to be proportional to the second and third cases in Table 1 and, therefore, don't represent a real new alternative to the cases already proposed.

On the other hand, the information coming from a sensor can be integrated, thus simulating a sensor of lower derivative. Following this idea, the cases of single integration of velocities and accelerations to get positions and velocities, respectively, and of double integration of accelerations to get positions, have been included in the study too. Of course, the

corresponding Jacobians of the measurement functions, $\mathbb{C}$, are again the same that those appearing in Table 1. The trapezoidal rule has been used to integrate the sensor data.

5 RESULTS AND DISCUSSION

For each case of those described in the previous section, the simulation of the prototype is first run, and the corresponding readings from the sensor stored. Then, the simulation of the model is launched, getting the stored readings of the prototype's sensor in order to calculate the EKF corrections. Each case is simulated for two fixed time-steps of integration, Δt=1 ms and Δt=10 ms. For each simulation, the covariance of the measurement noise, Ξ=diag(r), is adjusted so as to provide the best possible behavior of the observer, and CPU-time and error are obtained as results. In order to evaluate the error, the history of coordinate x_1 is stored for both the prototype and the observer, and the norm of the difference vector calculated in 101 points equally spaced in the interval of simulation is obtained,

$$e = \sqrt{\sum_{i=1}^{101} \left(x_{1,prot}^{i} - x_{1,obs}^{i} \right)^2} \tag{20}$$

The results for the cases shown in Table 1 are gathered in Table 2.

Sensor	RMS	Δt=1 ms			Δt=10 ms		
		r	CPU-time (s)	e (m)	r	CPU-time (s)	e (m)
θ	0.220	0.01	1.37	0.1669	0.01	0.16	0.1728
$\dot{\theta}$	2.049	0.01	1.38	0.2331	0.1	0.17	0.2708
$\ddot{\theta}$	24.06	100	2.82	0.2505	100	0.34	0.2566
y_1	0.187	0.01	1.37	0.2039	0.01	0.16	0.2040
$\dot{y}_1$	1.748	0.01	1.40	0.2835	0.1	0.17	0.3047
$\ddot{y}_1$	20.61	1000	1.91	0.2971	1000	0.23	0.2974

Table 2: Results for direct use of sensor measurement.

Now, the cases in which the sensor measurement is integrated once or twice in order to get lower derivatives are shown in Table 3.

Original sensor	# of integr.	Equivalent sensor	Δt=1 ms			Δt=10 ms		
			r	CPU-time (s)	e (m)	r	CPU-time (s)	e (m)
$\dot{\theta}$	1	θ	0.01	1.23	0.1672	0.01	0.15	0.1712
$\ddot{\theta}$	2	θ	0.01	1.25	0.1671	0.01	0.14	0.1708
$\ddot{\theta}$	1	$\dot{\theta}$	0.01	1.28	0.2355	0.1	0.14	0.2662
$\dot{y}_1$	1	y_1	0.01	1.25	0.2033	0.01	0.14	0.2044
$\ddot{y}_1$	2	y_1	0.01	1.23	0.2031	0.01	0.14	0.2051
$\ddot{y}_1$	1	$\dot{y}_1$	0.01	1.27	0.2811	0.1	0.14	0.3015

Table 3: Results for integrated sensor measurement.

To let the reader appraise the meaning of the errors gathered in Tables 2 and 3, Figure 3 shows the histories of coordinate x_1 and its derivative $\dot{x}_1$ for the prototype and the observer, for the cases with minimum and maximum error, respectively.

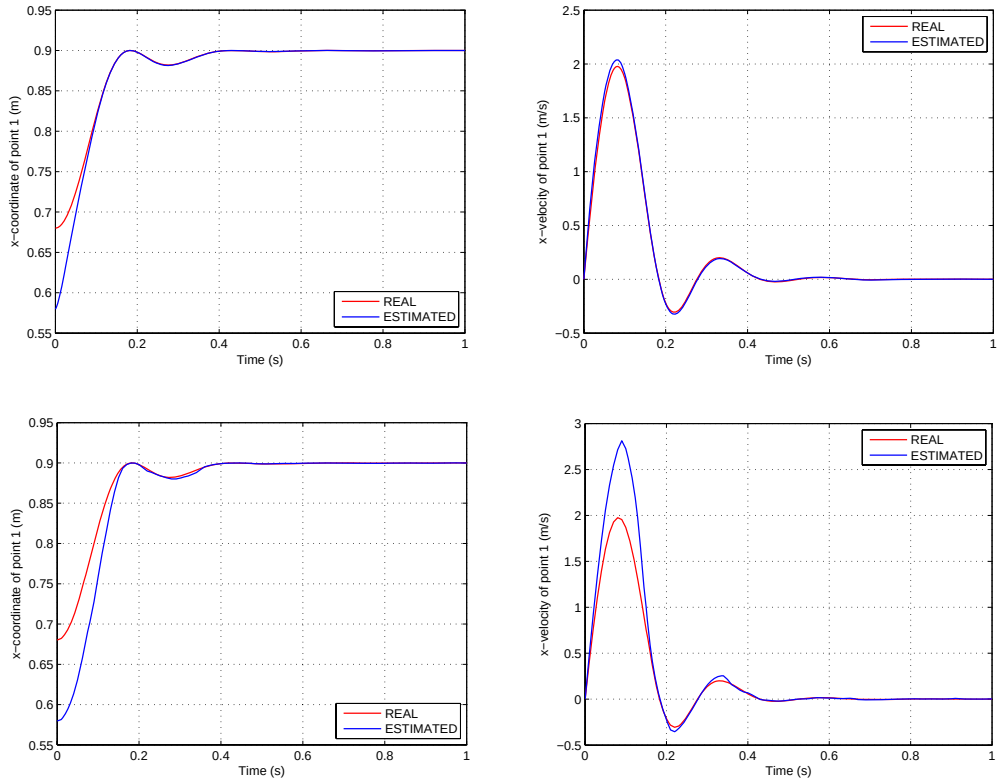

Figure 3: Histories of x_1 and $\dot{x}_1$ for prototype and observer: min error (0.1669) and max error (0.3047).

At the view of the results, it can be affirmed that the observer achieves to follow the prototype in all the cases, not only with the moderate time-step size of 1 ms, but also with the large time-step size of 10 ms. Therefore, good robustness properties have been obtained.

It is also clear that measuring velocities or accelerations leads to greater errors than measuring positions. Moreover, when acceleration sensors are used, the efficiency is notably reduced, and a huge increment of the covariance of the measurement noise is required in order to keep the stability of the observer.

In what respects to the type of variable measured, better results are obtained when the measured magnitude is the generalized coordinate of the problem, since the output Jacobian matrix $\mathbf{C}$ is more exact in that case.

Integration of the measured data to yield lower derivatives has shown to produce excellent results. Single integration of velocities or accelerations to get positions or velocities keeps the same error that the direct use of position or velocity sensors, respectively, and improves efficiency. The same trend is observed when accelerations are integrated twice to give positions. This behavior is attributed to the filtering effect caused by the trapezoidal rule during the integration process, which attenuates the noise level of the signal.

6 CONCLUSIONS

In this work, the influence of the sensored magnitude in the performance of the observers based on detailed multibody models and the extended Kalman filter has been studied. A four-bar mechanism has been chosen as example. Two computational versions of the mechanism have been created, the real “prototype” and the “model”, each one having different initial conditions and gravity value. Moreover, signals coming from the prototype sensors have been corrupted by a random noise. The behavior of the developed formalism, which relies on the

state-space reduction method known as matrix-R, has been analyzed for different sensored magnitudes -position, velocity, acceleration-, and for the cases when the sensored magnitude is or is not a generalized coordinate of the problem.

Based on the obtained results, the following conclusions can be drawn:

- The observer becomes less stable, accurate and efficient as higher derivatives are measured, thus demanding either to reduce the integration time-step or to increase the value of the measurement noise covariance in order to keep an acceptable behaviour.
- Anyway, the observer was able to deliver good results for time-steps as large as 10 ms in all the cases.
- The observer is less accurate if the sensored variable is not a generalized coordinate of the problem, since the output Jacobian matrix is less exact in that case.
- Integration of the sensor data to simulate the measurement of a lower derivative yields excellent results, likely due to the filtering effect of the integration process.

Therefore, it is expected that robust, efficient and accurate observers can be obtained for complex industrial systems, like cars, by combination of detailed multibody models and the extended Kalman filter. Such a study will be the subject of future research.

ACKNOWLEDGEMENTS

This work has been supported by the project "Desarrollo de un sistema ICC (Integral Chassis Control) con observador de estados" (07DPI005CT), granted by the Galician government to the Automotive Technological Center of Galicia (CTAG), and by the project DPI2006-15613-C03-01, granted by the Spanish government.

REFERENCES

[1] B. Ozkan, D. Margolis, M. Pengov. The controller output observer: Estimation of vehicle tire cornering and normal forces. *Journal of Dynamic Systems, Measurement, and Control*, **130**, 061002/1-062002/10, 2008.

[2] J. Cuadrado, D. Dopico, A. Barreiro, E. Delgado. Real-time state observers based on multibody models and the extended Kalman filter. *Journal of Mechanical Science and Technology*, DOI: 10.1007/s12206-009-0308-5, 2009.

[3] A.E. Bryson, Y.-Ch. Ho, *Applied optimal control. Optimization, estimation and control*. Wiley, New York, 1994.

[4] J. Garcia de Jalon, E. Bayo, *Kinematic and dynamic simulation of multibody systems*, Springer-Verlag, New York, 1994.